Volume 13 Article 11

2024

Postweaning Skull Growth in Living Didelphid Marsupials: The Case of Gracilinanus agilis and Cryptonanus chacoensis

Iveth A. Villalobos Guerrero
DePaul University, avilla46@depaul.edu

Noé U. de la Sancha
DePaul University, n.de.la.sancha@depaul.edu

Postweaning Skull Growth in Living Didelphid Marsupials: The Case of *Gracilinanus agilis* and *Cryptonanus chacoensis*

Iveth Adriana Villalobos Guerrero*

Department of Science and Health

Noé U. de la Sancha, PhD; Faculty Advisor

Department of Environmental Science and Studies

ABSTRACT Ontogeny is described as the history of an organism through its lifetime including development, growth, and allometry. The ontogenetic approach in cranial dimensions has proved useful in interpreting evolutionary patterns. Among the largest Didelphidae family of Neotropical marsupials, the species of *Gracilinanus agilis* and *Cryptonanus chacoensis* are poorly known. In this study, we address three questions; Is there sexual dimorphism in these species? What is the pattern of allometry? Which allometric patterns best describe the patterns in the skull and mandible? We applied geometric morphometrics to describe and test these differences using MorphoJ. A discriminant function analysis was performed to explore the comparisons between males and females on the ventral, dorsal, lateral, and mandible views of the skull. The analysis included the difference between means using the Mahalanobis and Procrustes distance, and permutation tests (n = 1000 permutation runs). Evidence of sexual dimorphism in *G. agilis* was not found, contrary to *C. chacoensis* where males and females differ the most at the parietal, occipital, and width of the temporal bones, the corpus, and three processes of the ramus. Age dimorphism was found in the cranium and mandible of both species, where the adults and juveniles differed the most in the parietal and occipital bones, the corpus, and the three processes of the ramus. In summary, we are closing the gap between two poorly understood species in South America. These findings will be important to better understand the ecology and evolution of these marsupials and other closely related species.

* *Avilla46@depaul.edu*

Research Completed in Winter 2024

INTRODUCTION

Didelphidae is the largest family of Neotropical marsupials occupying a wide variety of regions, ecoregions, and biomes including various forest types, grassland, and open habitats (Pacini and Harper 2008; Chemisquy et al. 2021; Astúa and Guilhon 2022). It has also been suggested that this family is characterized by a conservative morphology, which is a function of constraints in reproduction and development that limit their achievable final form (Eisenberg and Wilson 1981; Astúa de Moraes et al. 2000). Didelphids have been of special interest in research regarding the origin of their variation in shape given their range of ecological specialization and their morphology (Astúa de Moraes et al. 2000). The skull of Didelphid marsupials, as in all mammals, is expected to be closely associated with their ecology, in particular their trophic levels, thus the shape of their skulls is known as a reliable predictor of feeding ecology for the non-herbivorous species (Wroe and Milne 2007). A great variety of their specialized cranial structures are under selective pressure (Flores et al. 2023), and their skull is also less prone to vary and respond to directional selection due to their highly integrated skulls (Flores et al. 2023). The skulls depend on evolutionary forces that affect the relationship between form and function and thus are interesting as they further our knowledge of the ways these species perceive their environment and result in the specific properties of their morphology, for example, their masticatory apparatus (Flores et al. 2023). Studies in shape variation in Didelphidae can be traced back about 100 years when researchers focused on studies of biogeographic variation, comparative morphology, phylogenetic relationships, and morphometric analysis within species, and between sexes (Gardner 1973; Fonseca and Astúa 2015; Damasceno and Astúa 2016; Sebastião and Marroig 2013; Ventura et al. 2002; Astúa 2015; Astua 2010). Up until most recent years, a vast majority of these studies did not relate variation in shape to function with only a few exceptions. Due to this lack of study, specific characteristics of species within Didelphidae are still unknown.

Ontogeny is described as the history of an organism through its lifetime separated into three parts: development, growth, and allometry (Klingenberg 1998). Development is the organism's change in shape as a function of age, growth is the change in size as a function of age, and allometry is the change in shape as a function of size (Klingenberg 1998). The identification of ontogenetic patterns is relevant to the study of morphological changes in species as it gives us an insight into their variability which is based on ontogenetic changes (Klingenberg 1998). The description of this process is provided by the comparison of shapes in static stages (Klingenberg 1998). The study of ontogenetic patterns can identify the geographic, interspecific variation of species, and/or their ontogenetic variability, which is especially important for species that show morphological seasonal fluctuations (Hernandez et al. 2017). If ontogenetic variation is not taken into account, complications may arise where the comparisons are related to age variants, rather than to the taxonomic units of each species (Hernandez et al. 2017). This can create conflicts of comparison within the taxonomic or ecological patterns (Voss and Jansa 2009).

The ontogenetic approach in the study of cranial dimensions has proved useful in interpreting evolutionary patterns (Flores et al. 2022). This has not only demonstrated that a phylogenetic legacy influences the changes occurring during the development of species but also has shown the influence of the natural history of the species on their diet and feeding habits (Segura 2015). Thus, multiple perspectives such as descriptive, functional, and evolutionary aspects of morphology have been studied in marsupials (Weisbecker et al. 2008; Flores et al. 2018), including postnatal and post-weaning cranial ontogeny of Australian and New World marsupials (Abdala et al. 2001; Giannini et al. 2004; Flores et al. 2006, 2013, 2015, 2018).

Traditional and geometric morphometrics are the most widely used techniques as these quantitatively analyze the ontogenetic patterns of skulls (Segura et al. 2013; Hernandez et al. 2017). The difference between these approaches lies in their methodology, where traditional morphometrics use linear distances and angles while geometric morphometrics are based on the

homologous landmarks on cartesian coordinates (Adams and Nistri 2010; Zelditch et al. 2012; Klingenberg 2016; Hernandez et al. 2017). The main difference between these approaches lies in the way the shape of the subjects is analyzed. In geometric morphometrics, the shape is defined by the configuration of morphological landmarks where homologous landmarks are superimposed, rotated, and scaled, by a process known as Procrustes Superimposition. This is different from linear morphometrics where the shape is defined by the distances between the morphological configuration (Klingenberg 1998). Due to this, geometric morphometrics provides a fundamental tool that visualizes shape differences among group members (Astúa de Moraes et al. 2000). Nonetheless, not many studies have applied both linear and geometric morphometrics approaches to the same subjects, where the ones that have done it showed that the results were concise between both approaches (Hernandez et al. 2017). Statistically, different approaches of analysis such as bivariate and multivariate (where the ontogenetic trajectories of skull growth are analyzed) have been applied to the study of ontogeny in a variety of species (Segura 2015). Similarly, the two-dimensional geometric morphometrics approach has been applied to study the relationship between different ontogenetic qualities such as feeding performance, biomechanical performance, and dentition variation (La Croix et al. 2011a; b). On the other hand, the three-dimensional geometric morphometrics approach has been applied to study skull morphology where heterochronic patterns are analyzed (Drake 2011).

The species within the genus *Gracilinanus* (usually found in tropical and subtropical forests within lowland and montane landscapes in countries such as Venezuela, Bolivia, Paraguay, Brazil, Argentina, and Uruguay) and *Cryptonanus* (usually found in a range of tropical to temperate latitudes) have not been studied much (Flores et al. 2022). Historically, the species in the genus *Cryptonanus* were included within *Gracilinanus* until the systematic revision by Voss et al. (2005). The use of traditional morphometrics on *G. agilis* and *Cryptonanus spp*. include multivariate analyses of craniodental traits which revealed that adult samples of both species are distinguishable based on generally distinct craniodental and post-cranial characters (Voss et al. 2005) and size (Garcia et al. 2010). Other than traditional morphometrics where ontogenetic changes are not defined (Voss et al. 2005), cytogenetics has also been applied to *G. agilis* and some *Cryptonanus species* (Garcia et al. 2010). Geometric morphometrics as a rising area of study has barely been used in both genera. Furthermore, it has been a continuous problem to distinguish specimens of similar size but different ages of *G. agilis* from species of *Cryptonanus spp.* using traditional morphometrics (Garcia et al. 2009). This stands as one of the reasons behind the lack of morphometric analysis within these genera (Garcia et al. 2010). Other problems include the semelparity nature of both populations as well as the recollection of specimens where usually these have not been collected simultaneously (Voss et al. 2005).

Among the didelphids marsupials, small mouse opossum ontogenetic variation has been poorly studied. While recent research has been focused on identifying specifics such as sexual dimorphism within species, their ontogeny has been disregarded as a cause of such results (Astúa de Moraes et al. 2000). Consequently, using geometric morphometrics in the study of ontogenetic and allometric development of *G. agilis* and *C. chacoensis* functions as an effective method to identify the possibilities of age and sexual dimorphism regardless of their size while exploring the causes and consequences of development. In this regard, using comparative interspecific studies on allometric variation could improve and further the analysis and knowledge of both species in the study of their ontogenetic development. This would allow us to note the effects of the role these species play in the ecosystem. In this study, we address three specific questions: Is there sexual dimorphism in these species? What is the pattern of allometry? Which of these allometric patterns best describes the patterns in the skull and mandible? The answer to these questions would allow us to further develop our understanding of the biodiversity of species, to fill up the ontogeny gap of knowledge and the consequence and impact of their loss in the ecosystem.

METHODS

In this study, specimens from two species including 22 *Gracilinanus agilis* and 17 *Cryptonanus chacoensis* were analyzed. The specimens were collected during sampling to understand small mammal biodiversity (de la Sancha 2014; de la Sancha et al. 2023, Boyle et al. 2021) from December 2006 to March 2009 in Limoy Biological Reserve, Mbaracayú Natural Forest Reserve, Morombí Natural Private Reserve, and San Rafael Managed Resource Reserve (de la Sancha 2014). All the specimens can be found in the mammal collection of the Field Museum of Natural History (FMNH), in Chicago, Illinois.

The specimens sampled included both females and males, ranging from juveniles to adults. Both the *G. agilis* and the *C. chacoensis* were categorized into one of six dental age classes, based on molar eruption and molar wear sensus Tribe (1990). For our *C. chacoensis* specimens only classes 6 and 3 were identified, while the specimens of *G. agilis* variated between classes 3, 6, and 7. Dorsal, lateral, ventral, and mandible faces were photographed with an Olympus Tough TG-6 Camera with a 2x Optical Zoom. The plane of the lens was parallel to the base of a copy stand. This standardization of the camera to the specimens was necessary to avoid any deformations due to the lens along the outer edges of pictures. The lateral and mandible sides of the specimens' crania were standardized at a fixed orientation using a box full of black sand as a holder, and the dorsal and ventral views of the specimens' crania were standardized by resting them on rubber bands following Hernandez et al. (2017). This was established so that the same structures supported both species to minimize the deviations in orientation angles. The camera was mounted on a stand at a fixed distance with a depth of 12 cm from the rubber band's box, and 11 cm from the box of sand. The distance being fixed ensured that the scale was consistent for all analyses of size variation.

Landmarks were digitized on pictures to identify homologous structure variations in specific parts of the cranium and the mandible (Fig. 1 and 2). The same number and proper position of landmarks were used in the digital images of both species (see Appendix A for the description of landmarks). 14 landmarks were positioned on the lateral and ventral sides of the cranium, 11 on the dorsal side of the cranium, and 19 landmarks in the mandible. (Figures 1 and 2) using the TpsDig2w32 software (Rohlf 2015). The landmarks were positioned on just one-half of all sides of the cranium and the mandible to avoid symmetry issues and inflation of error terms (Cardini 2016). In areas where one specific landmark was missing, the coordinates from the opposite side were used to place the missing landmark instead of using average coordinates (Astua 2010). The landmarks used were chosen to describe the variation in the cranial development of both specimens.

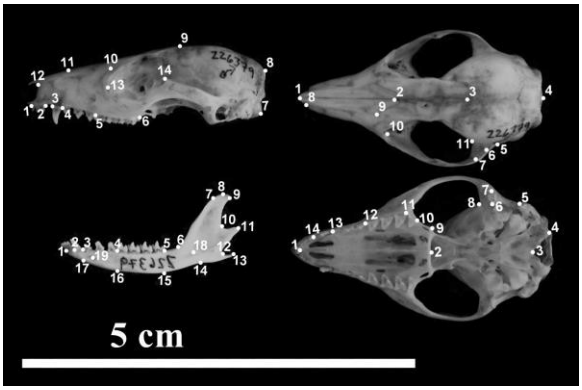

Figure 1. Location of landmarks on the four views of the skull of *Gracilinanus agilis*. Landmark descriptions are presented in Appendix A.

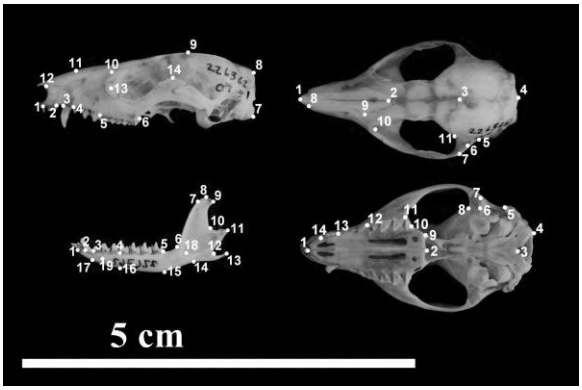

Figure 2. Location of landmarks on the four views of the skull of *Cryptonanus chacoensis*. Landmark descriptions are presented in Appendix A.

A multivariate framework was used to quantify shapes and patterns of change using geometric morphometrics following Hernandez et al. (2017).

All specimens were first subjected to a Generalized Procrustes fit analysis which aligned, rotated, and scaled all homologous landmarks. A covariance matrix was generated using the Procrustes coordinates (Adams and Otárola-Castillo 2013). The specimens were then compared based on their age, sex, and dental class groups using the MorphoJ software.

Principal component analyses (PCA) were performed using the Procrustes coordinates to explore the different patterns that arise from the shape variation and to determine the differences in shape between the age classes, the age, and the sex of both species. Discriminant function analyses (DFA) were then performed to explore the comparisons between males and females on all four views of the cranium (ventral, lateral, dorsal, and mandible). The analysis included the difference between means using the Mahalanobis and Procrustes distance, and the p-value for the permutation test (n = 1000 permutation runs) using Procrustes distance and the T-square values (Hernandez et al. 2017).

Similarly, DFA (also known as canonical variate analysis (CVA) for more than two groups (Strauss 2010) was then applied to the aligned coordinates to analyze the shape differences between the sex, age, and class groups to find the greatest axes of variation using MorphoJ. Subsequently, the DFA was followed up with permutation tests, with 5000 iterations, on the four views of the cranium of both species to evaluate the global test against the null hypothesis of no difference among groups between the canonical coefficients for the sex, age, and the class groups. Allometry was quantified by a Procrustes allometric regression analysis (n = 10000 iterations) performed on Morpho J to analyze the shape co-variation data to compare the Procrustes allometric score with the log-transformed centroid size of all the specimens (Hernandez et al. 2017). The total number of images used in the analysis for each species including species name, side of the cranium, and sex are listed in Table 1.

Species	Ventral Total		Dorsal Total		Lateral Total		Mandible Total	
	M	**F**	**M**	**F**	**M**	**F**	**M**	**F**
Gracilinanus agilis	22		22		22		22	
	10	12	10	12	10	12	11	12
Cryptonanus chacoensis	17		17		17		17	
	7	10	7	10	7	10	7	10

Table 1. Number of images used in analysis per species for each view where M = males and F = females.

RESULTS

Principal Component Analysis

The PCA analysis, the eigenvalues, and their percentage of variance for all four views on both species are given in Table 2 and Figure 3 where PC1 explained the vast majority of variance on all sides of the cranium for both species.

Specie	PC	View	Eigenvalues	% Variance
Gracilinanus agilis	PC1	Dorsal	0.0007122	50.38%
		Mandible	0.0007941	45.95%
		Lateral	0.0003850	29.68%
		Ventral	0.0004627	41.92%
	PC2	Dorsal	0.0002518	17.81%
		Mandible	0.0002048	11.85%
		Lateral	0.0002373	18.30%
		Ventral	0.0003077	27.87%
Cryptonanus chacoensis	PC1	Dorsal	0.0009692	56.45%
		Mandible	0.0009357	46.20%
		Lateral	0.0007969	29.66%
		Ventral	0.0005583	47.61%
	PC2	Dorsal	0.0002592	15.09%
		Mandible	0.0003305	16.32%
		Lateral	0.0005585	20.79%
		Ventral	0.00026641	22.72%

Table 2. Results of the principal component analysis for PC1 and PC2 on all views of *G. agilis* and *C. chacoensis.*

On all four views of the skull for each species, PC1 had the strongest variance in the dorsal view on both *G. agilis* and *C. chacoensis* with percentages of 50.38% and 56.45% respectively, and the second strongest variance on the mandible of *G. agilis* and ventral view of *C. chacoensis*. In comparison, PC2 explains the strongest variance in the ventral side of the skull of both *G. agilis* and *C. chacoensis* with percentages of 27.87% and 22.72% respectively, and the second strongest variance in the lateral view of both *G. agilis* and *C. chacoensis*. The PC scores from the PCA analysis for *G. agilis* and *C. chacoensis* varied by which landmarks

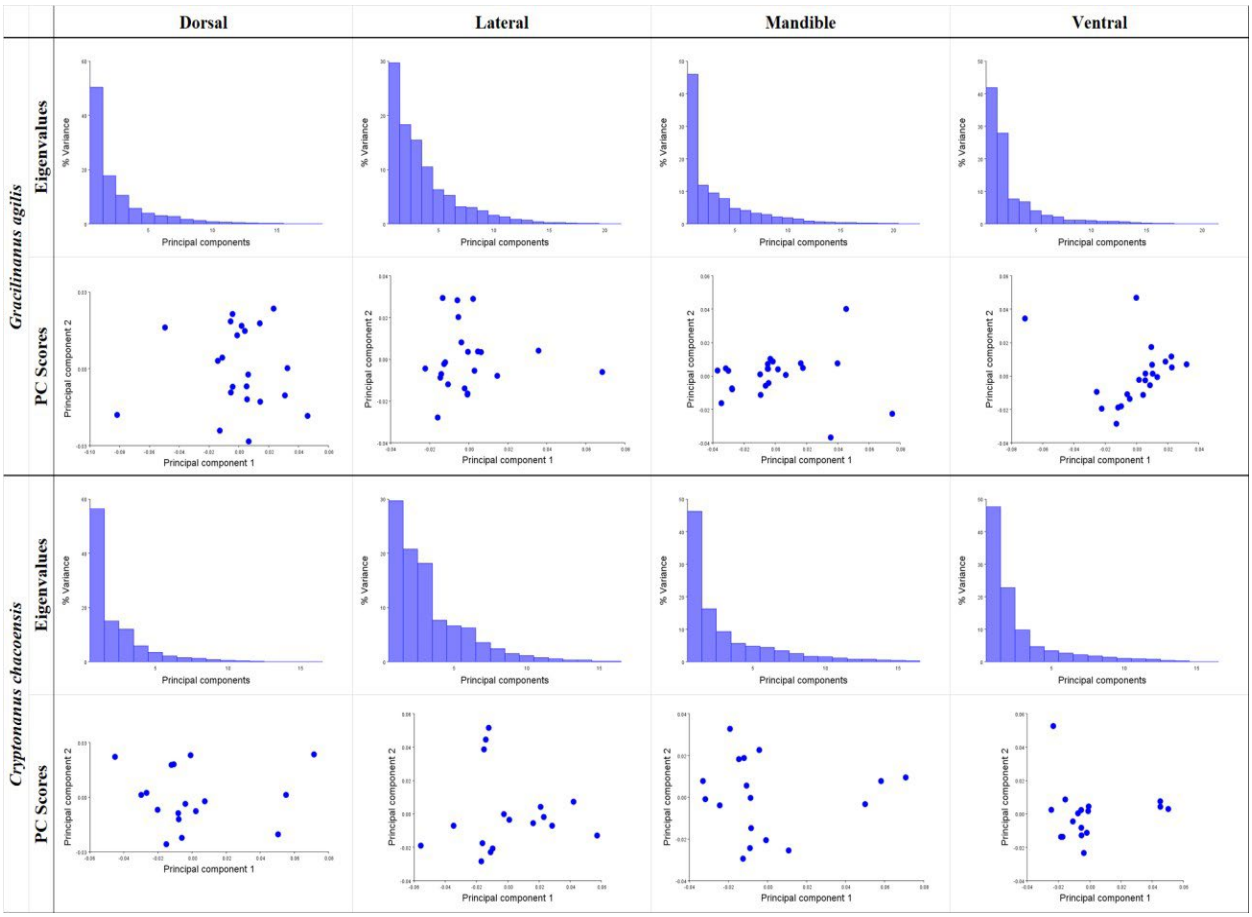

Figure 3. Results of the PCA analysis including Eigenvalues and plot of the first two PC scores from the dorsal, lateral, mandible, and ventral sides of the skull of *G. agilis* and *C. chacoensis.* Values are detailed in Table 2.

captured most of the cranial variation (Figures 3-5). *G. agilis* had a lower shape variation overall (Figure 4) in comparison to *C. chacoensis* (Figure 5).

All the other views of *G. agilis* and *C. chacoensis* seem independent of each other. Regardless of the correlation between the four views for each species, the value's importance was applied to the PC1 and PC2 loadings (Appendix B) where in the dorsal view of *G. agilis*, PC1 was highly related to the overall length of the skull (landmarks 2, 4, 8, and 9), while PC2 was related to the posterior part of the zygomatic arch (landmark 5) and the junctional suture in between the frontal and parietal bones of the cranium (landmark 3). In the mandible, PC1 was highly related to the vertical posterior line at M4 (landmarks 5 and 15), while PC2 was related to the vertical anterior line at M1 (landmarks 4 and 16), and the beginning of the ramus (landmark 18). In the lateral view, PC1 was highly related to the width of the cranium from the dorsal to the ventral side (landmarks 6, 9, and 14) while PC2 was related to the medial to dorsal width of the cranium (landmarks 9 and 14) and the anterior end of the zygomatic arch (landmark 6). Finally, in the ventral view, PC1 was highly related to the anterior end of the foramen magnum (landmarks 3), the posterior end of the zygomatic arch (landmark 8), and the anterior end of the zygomatic arch found in between the orbitals (landmark 11), while PC2 was related to the posterior end of M4 (landmark 10). On the other hand, in the dorsal view of *C. chacoensis*, PC1 was highly related to the overall length of the cranium (landmarks 1, 2, 3, and 4) while PC2 was related to the junctional suture in between the frontal and parietal bones of the cranium (landmarks 3) and the suture between the nasal bone, the frontal bone, and the maxilla (landmark 9). In the mandible, PC1 was highly related to the inferior and anterior part of the ramus (landmark 15) and the posterior end of M4 (landmark 5), while PC2 was related to the overall length of the ramus (landmarks 9, 14, and 15). In the lateral view, PC1 was highly related to the posterior end of M4 (landmark 6) and the superior view around the nasal bone (landmark 11), while PC2 was related to the inferior end of the foramen magnum (landmark 7), the superior end of the cranium around the frontal bone

(landmark 9), and the peak area of the zygomatic arch (landmark 14). Finally, in the ventral view, PC1 was highly related to the anterior part of the foramen magnum (landmark 3), the posterior view at the beginning of the zygomatic arch within the orbitals (landmark 8), the posterior end of M4 (landmark 10), and the anterior end of M1 (landmark 12), while PC2 was related to the incisors (landmark 1) and the left end of the foramen magnum (landmark 4). The description of the landmarks is given in Appendix A.

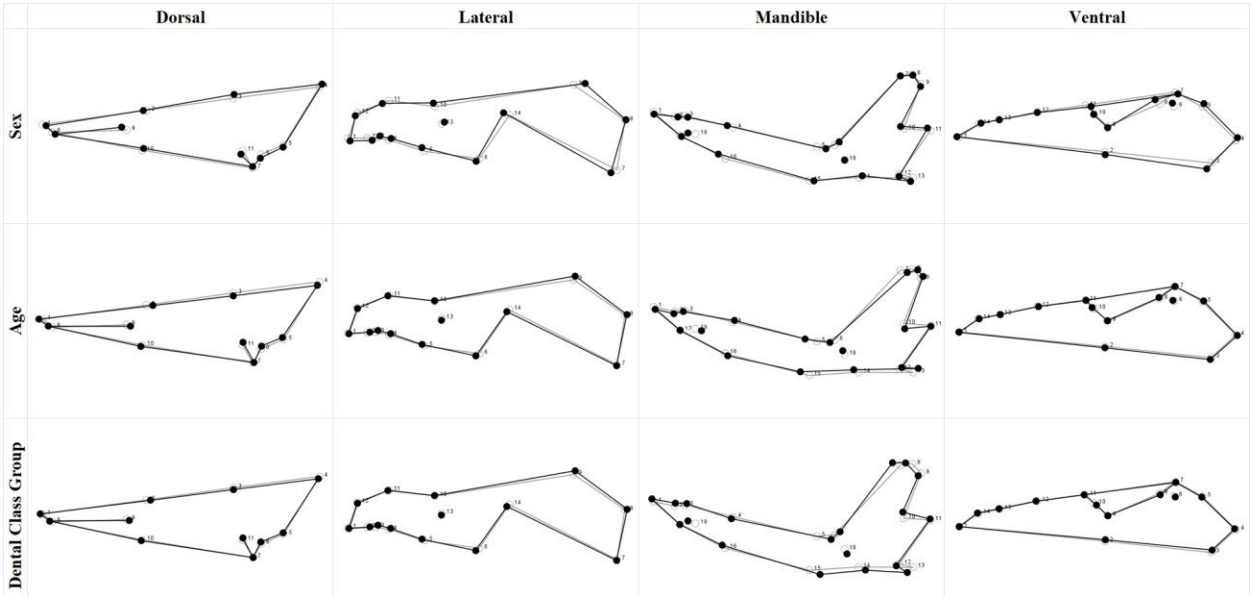

Figure 4. Shape variation of the cranial and mandible views via wireframe of *Gracilinanus agilis* based on discriminant function analyses including differences between sex, age, and dental class (see Figure 1 for views and text for detailed descriptions of groups). Grey outline on all sides of the skull: adult male of class 6.

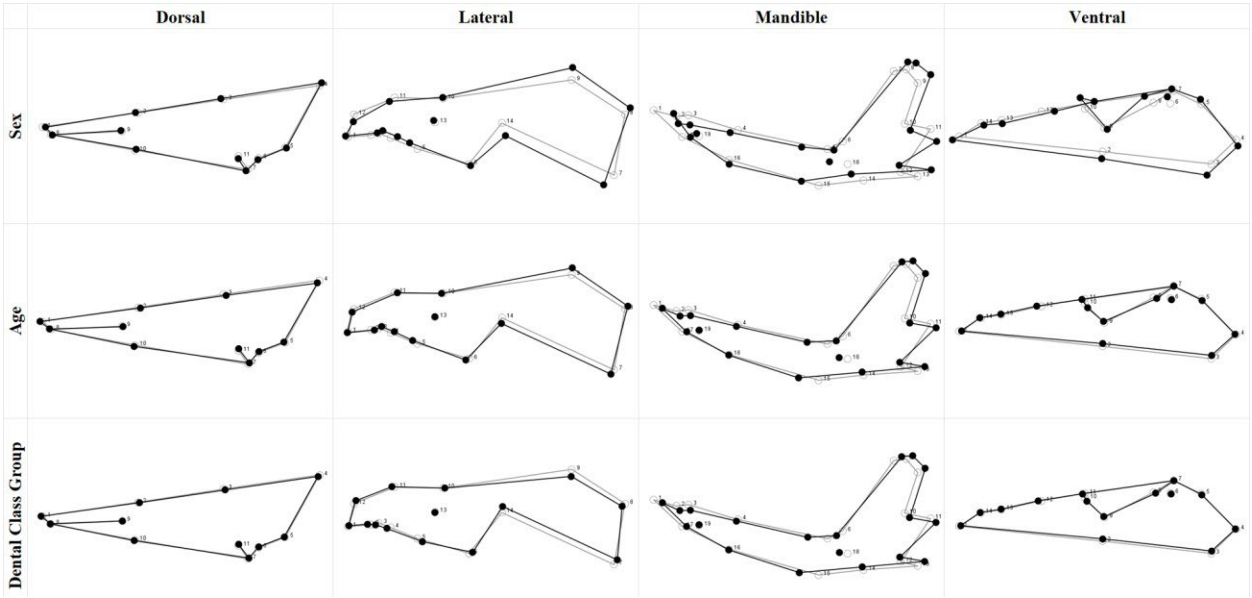

Figure 5. Shape variation of the cranial and mandible views via wireframe of *Cryptonanus chacoensis* based on discriminant function analyses including differences between sex, age, and dental class (see Figure 2 for views and text for detailed descriptions of groups). Grey outline on all sides of the skull: juvenile female of class 3.

Sexual Dimorphism Discriminant Function Analysis

Permutation tests for Procrustes and Mahalanobis distances did not find significant differences (P>0.05) between males and females for all four views. (Table 3, Figure 6). Similarly, the results from the p-values for permutation tests on all four views of the *G. agilis*, and the lateral and mandible views of the *C. chacoensis* do not show a significant difference on the Procrustes distance with a P > 0.05, whereas the dorsal and ventral views of the *C. chacoensis* do show a significant difference where P < 0.05 (Table 4).

Specie	View	Procrustes Distance	Mahalanobis Distance	P-value (Parametric)
Gracilinanus agilis	Dorsal	0.02	4.80	0.57
	Mandible	0.02	3.77	0.97
	Lateral	0.02	3.31	0.98
	Ventral	0.01	3.22	0.99
Cryptonanus chacoensi	Dorsal	0.04	14.3	0.39
	Mandible	0.03	2.23	1.00
	Lateral	0.03	3.38	0.95
	Ventral	0.03	2.98	0.97

Table 3. Results of the discriminant function analysis from the difference between means on the male-female comparison of *G. agilis* and *C. chacoensis.*

Specie	View	Procrustes Distance	T-square
Gracilinanus agilis	Dorsal	0.215	0.552
	Mandible	0.356	0.105
	Lateral	0.108	0.656
	Ventral	0.457	0.759
Cryptonanus chacoensis	Dorsal	0.015	0.126
	Mandible	0.083	0.291
	Lateral	0.174	0.304
	Ventral	0.015	0.724

Table 4. Results of the discriminant function analysis and permutation tests (n=1000) on the male-female comparison of *G. agilis* and *C. chacoensis*

The cross-validation and discriminant scores between females and males on all four views of both species can be seen in Figure 6.

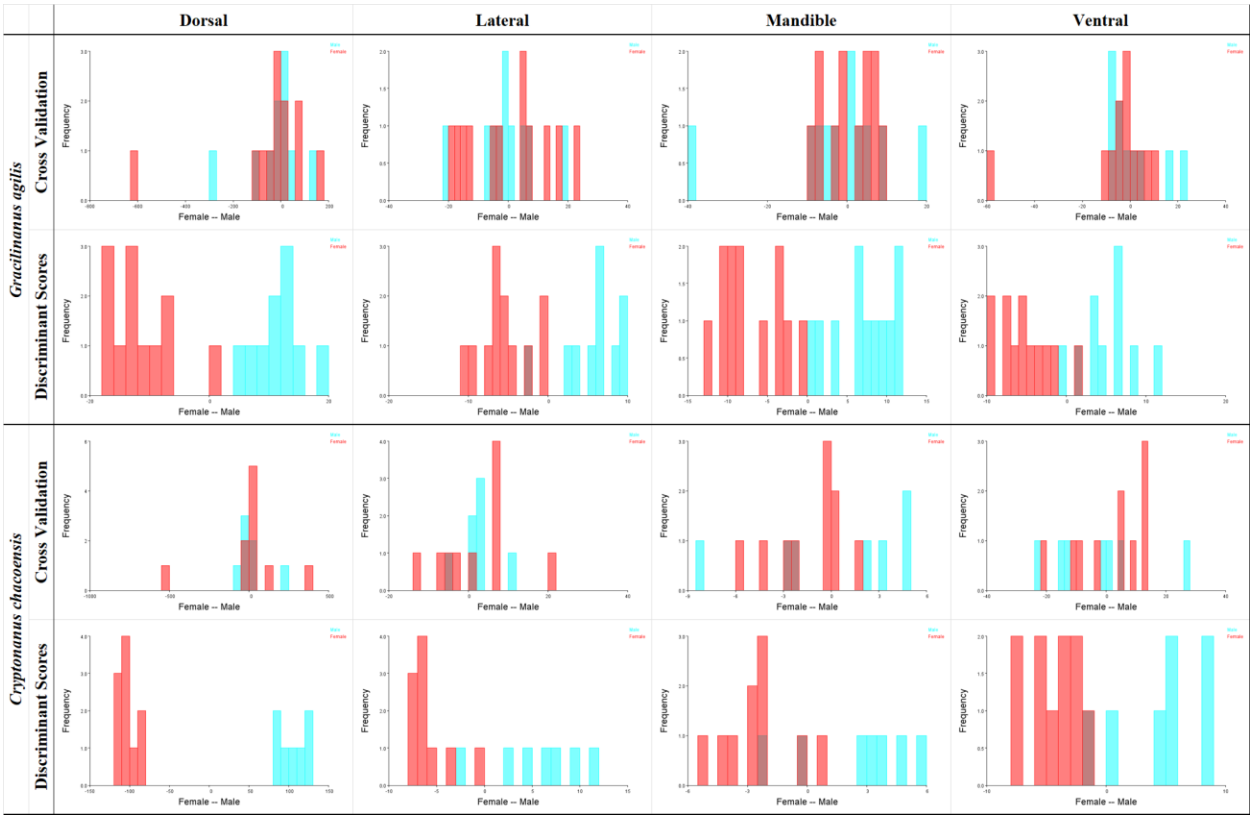

Figure 6. Results of the DFA analysis on the dorsal, ventral, and lateral sides of the cranium and mandible of *G. agilis* and *C. chacoensis* including the cross-validation analysis and discriminant scores.

Age-Based Discriminant Function Analysis

Results from the age based DFA to all four views on the *G. agilis* specimens showed no sexual dimorphism with a statistical significance of $P > 0.05$. This shows that the ontogenetic variation between males and females was the same, and the allometric patterns observed were not based on their sex. On the other hand, *G. agilis* did show an age and dental class dimorphism, with a statistically significant $P < 0.05$. Thus, their allometric patterns were dependent on these variables. On the other hand, all four views on the *C. chacoensis* specimens showed a statistically significant difference in sex, age, and dental class with a $P < 0.0001$ (Table 5). The results show a difference in ontogenetic variation dependent on all three factors (sex, age, and dental class groups). As both species showed different degrees of sexual dimorphism, the sexes and the species were analyzed separately.

Results of the canonical variance analysis on all four views for both species can be seen in Figures 7 and 8, where the age of *G. agilis* (Figure 7), and the age and dental class of *C. chacoensis* (Figure 8) are based on the relationship between the CV1 and CV2. On the other hand, the dental class and sex of *G. agilis,* and the sex of *C. chacoensis* are based on the relationship between the CV1 and the frequency. Although CV1 seems to be mainly driven by the age on the dorsal side of the cranium of *G. agilis*, CV2, and CV1 are relatively equally driven by the lateral, mandible, and ventral sides of the cranium of *G. agilis,* and on all four views on age and dental class of *C. chacoensis.*

Specie	View	Effect	Goodall's F	P-value
Gracilinanus agilis	Dorsal	sex	1.397	0.2222
		age	5.8688	0.0038
		class	9.5935	0.0036
	Mandible	sex	1.0286	0.3472
		age	5.0654	<.0001
		class	8.3435	0.0004
	Lateral	sex	1.5938	0.11
		age	4.3476	0.0004
		class	6.235	0.0008
	Ventral	sex	0.9334	0.4566
		age	7.5215	0.0018
		class	8.0409	0.0034
Cryptonanus chacoensis	Dorsal	sex	3.6003	<.0001
		age	7.177	<.0001
		class	6.9848	<.0001
	Mandible	sex	2.1352	<.0001
		age	5.7885	<.0001
		class	5.5935	<.0001
	Lateral	sex	1.4165	<.0001
		age	1.9196	<.0001
		class	2.3541	<.0001
	Ventral	sex	3.2178	<.0001
		age	6.0958	<.0001
		class	6.4875	<.0001

Table 5. Results of the canonical variate analysis and permutation tests (n =5000) on *G. agilis* and *C. chacoensis* for all four views.

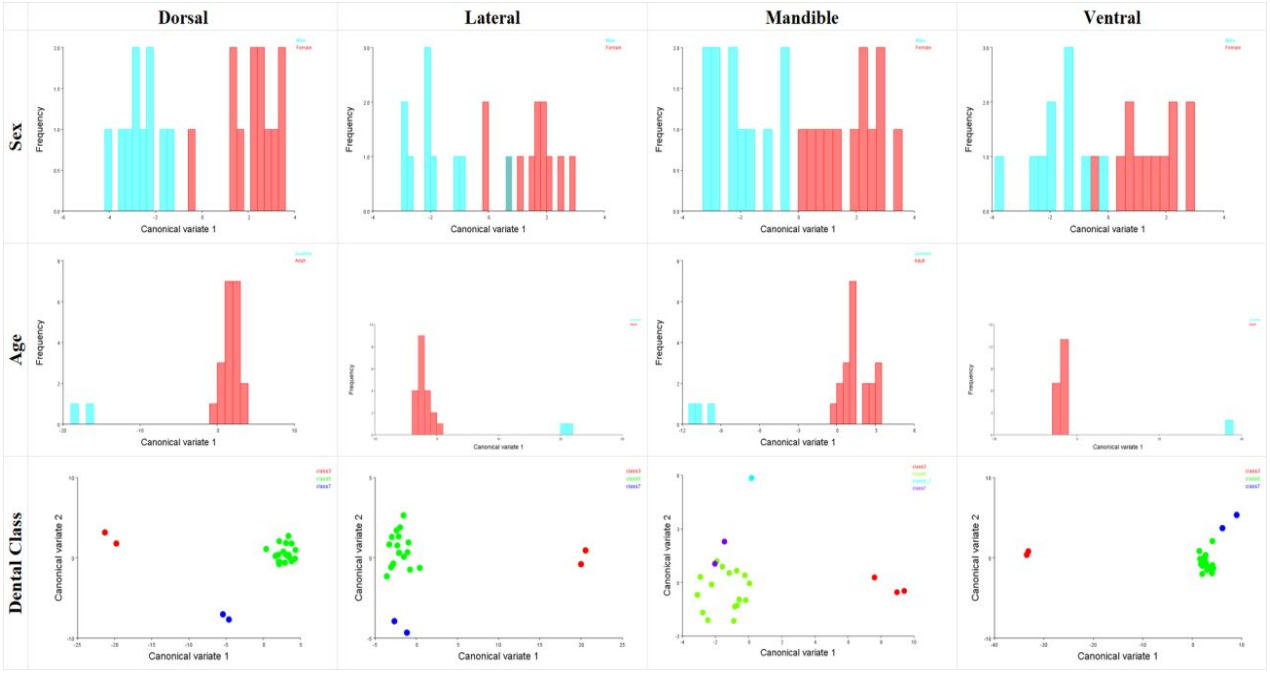

Figure 7. Results of the CVA analysis on sex, dental class, and age for all four views with graphs from *G. agilis*.

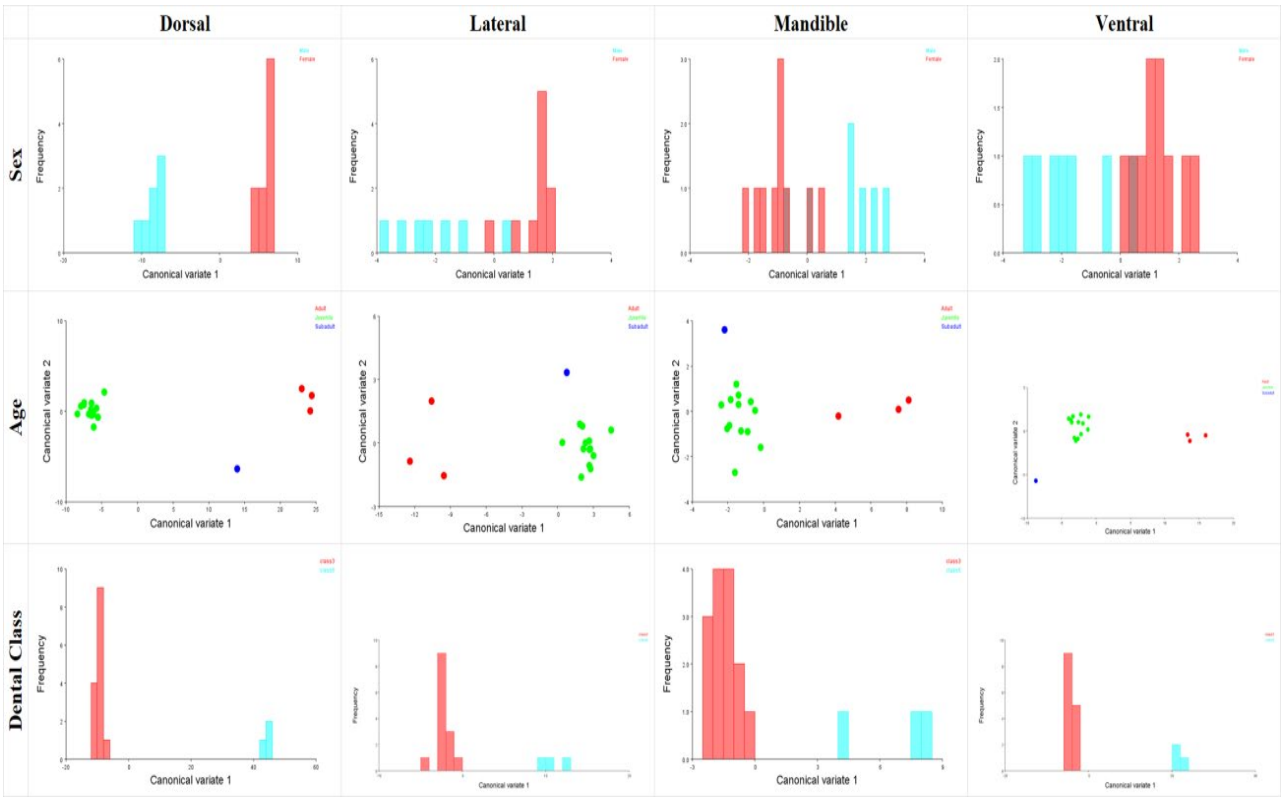

Figure 8. Results of the CVA analysis on sex, dental class, and age for all four views with graphs from *C. chacoensis.*

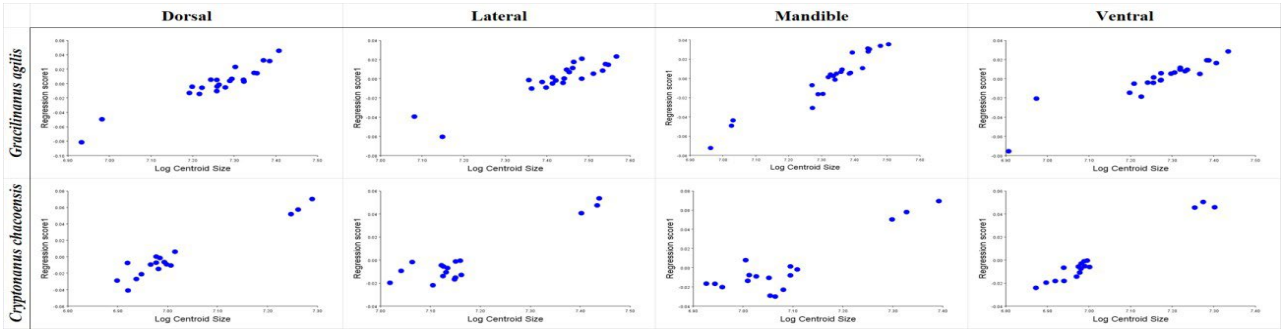

Figure 9. Results of the allometric regression analysis performed on all four views of A) *G. agilis* and B) *C. chacoensis*, where Procrustes coordinates were the independent variable and the Log Centroid size, was the dependent variable (n=10000).

Allometry

The results from the Procrustes allometric regression analysis performed on all four views for *G. agilis* and *C. chacoensis* with the Procrustes coordinates as the dependent variable, and the Log Centroid Size as the independent variable with a permutation test of 10000 rounds are given in Table 6 and Fig. 9. The results show that the positive allometric trends of change in shape as a function of size on all four views of both species were significant ($P < 0.005$).

Specie	View	P-value	% Predicted	Total SS	Predicted SS	Residual SS
Gracilinanus agilis	Dorsal	<0.0001	45.6%	0.030	0.014	0.016
	Mandible	<0.0001	41.4%	0.038	0.016	0.022
	Lateral	0.0001	23.1%	0.027	0.006	0.021
	Ventral	<0.0001	33.2%	0.023	0.001	0.015
Cryptonanus chacoensis	Dorsal	<0.0001	52.0%	0.027	0.014	0.013
	Mandible	0.0009	35.4%	0.032	0.011	0.021
	Lateral	0.0020	17.8%	0.043	0.008	0.035
	Ventral	<0.0001	46.1%	0.019	0.009	0.010

Table 6. Results of the Procrustes allometric regression analysis (n=10000) for all views on *G. agilis* and *C. chacoensis.*

Subsequently, the allometric trends based on the dorsal, mandible, and ventral view of *G. agilis*, and the dorsal and ventral view of *C. chacoensis* show that the positive trend of a change in shape as a function of size was highly significant

($P<0.0001$). On *G. agilis*, the size of the dorsal view predicted 45.6% of its shape, the size of the mandible predicted 41.4% of its shape, and the size of the ventral predicted 33.2% of its shape. On *C. chacoensis*, the size of the dorsal view predicted 52.0% of its shape, whereas the size of the ventral predicted 46.1% of its shape. These results as well as the total sum of squares (SS), the predicted (SS), and the residual (SS) are given in Table 6.

DISCUSSION

The conservative morphology of Didelphidae (and all other marsupials) has been suggested to be caused by its special reproductive and developmental characteristics (Pilatti and Astúa 2017). This group must be capable of being independent of the mother after a short period of gestation, where they should breathe and eat by themselves to survive (Maunz and German 1996; de Oliveira et al. 1998). During this period, their craniofacial morphogenesis is still developing, but their premaxillae, maxillae, palatine, and dentary bones are already in the process of being ossified (Abdala et al. 2001). This process is thus considered to impose certain constraints in the development of this group as it limits the final form they are to obtain, including the responses of the cranium and the mandible to the selection of their functional features (Eisenberg and Wilson 1981; Astúa de Moraes et al. 2000). Furthermore, the skull of these mammals is highly integrated and is related to foraging strategies (Flores et al. 2023). The specializations of its structure are under selective pressures that depend on evolutionary forces which usually act in a variety of directions where the form and function of the skull are expected to come from the strength of these forces (Flores et al. 2023). Nonetheless, the elements of the skull do not remain constant during development, which means that parts of the skull change independently from each other during growth (Smith 2006). This in consequence creates different degrees of integration of the skull (Smith 2006). Ontogenetic studies on carnivores and other mammals have shown that morphometric changes are related to the improvement of feeding and biting (Segura 2013). It has also been observed that there is a relationship between skull morphology, shape, and function (Garcia-Perea 1996; Segura and Flores 2009; Giannini et al. 2010; Flores and Barone 2012). Thus, by studying the shape and function, and in consequence, the allometry of these species during and after development, we can know the specific evolutionary forces that cause these specializations during different stages of development (Flores et al. 2023). This focus on allometry is important as it is known to be one of the main factors that lead to the cranial diversification that is usually found in Didelphidae (Flores et al. 2023). Due to the conservative morphology of this group as well as their specialization in a variety of ecosystems, the variation in the shape of this group is usually studied by comparing different ages, dental classes, species within the group, and their sexes (Pilatti and Astúa 2017; Maunz and German 1996; Clark and Smith 1993; Hernandez et al. 2017; Astúa 2015).

While species in these genera are very similar, they can be differentiated by the combination of characters in the skull including the second upper premolar which is shorter than the third upper molar in *Cryptonanus* and their upper canine counts with accessory cusps vs subequal and no cusps on in *Gracilinanus*; *Gracilinanus* has a paired maxillopalatine fenestrae and maxillary fenestrae in the palate, with the latter missing in Cryptonanus; and a secondary foramen ovale present in Gracilinanus and absent in Cryptonanus (Voss et al. 2005). Their rostrum is shorter and their orbits smaller in *Gracilinanus*, but these characteristics are known to be ontogenetically variable (Garcia et al. 2010). While these are qualitative characters, these and other variables were both directly and indirectly analyzed using the PCA analysis (see Figures 1 and 2 for placement of structures described in Appendix A). This showed that on *G. agilis* and *C. chacoensis*, most of the variance on the dorsal part of the cranium was due to the posterior end of the left and right junction of the nasal, and the posterior end of the interparietal bone on the intersection of the sagittal line with the nuchal crest. On the other hand, the variance on *G. agilis* was also dependent on the anterior end of the suture between the nasal bone and the premaxilla, and the intersection of the sutures between the

nasal and frontal bones, and the maxilla. On *C. chacoensis*, most of the variance was also due to the tip of the nasal, and the junction between the right and the left suture of the frontal and the parietal bones. The mandible of both species experiences the vast majority of variance in the posterior base of the inferior M4 where the teeth meet the dentary bone (very important on both species), and the parallel horizontal projection of this location on the ventral edge of the mandible (very important only in *G. agilis*). On the lateral view, both species experience the most variance in the posterior base of M4, where the tooth meets the maxillary bone (posterior end of the molar series). Nonetheless, *G. agilis* also experiences the vast majority of variance at the top of the sagittal crest where the frontal and parietal bones meet, and where the jugal bone's frontal process ends on the zygomatic arch. Meanwhile, *C. chacoensis* experiences the most variance on the junction between the nasal, the premaxillary, and the maxillary bone sutures. The vast variety on the ventral side of both species was dependent on the anterior-most point of the foramen magnum, and the point of maximum curvature on the anterior margin of the zygomatic process of the temporal bone. On the other hand, this side of *G. agilis* also experiences the most variance on the distal-most point between M3 and M4, while *C. chacoensis* experiences the most variable on the posterior-most end of M4 and the distal-most point between M1 and P3 (Figure 3, Table 2, Appendix B).

Among all marsupials, the Didelphidae family is known as one of the most carnivorous (or at least insectivorous). This is important since it has been documented that there are predominant differences in the musculature associated with biting apparatus related to food consumption especially compared to purely herbivorous species within the Diprotodontia and *Macropus* spp. (Coues 1872; Osgood 1921; Hiiemae and Jenkins 1969; Freeland and Janzen 1974; Smith 2006; Tomo et al. 2007; Fritz et al. 2009; Sharp 2015; Diogo et al. 2018). Furthermore, sexual dimorphism has been detected in *G. agilis* in other studies (Costa et al. 2003) which excluded smaller specimens. On the other hand, sexual dimorphism has never been tested on *C. chacoensis* (Garcia et al. 2010) until now. The results from my study of the canonical variate analysis of *G. agilis* (Table 5, Figures 4 and 7), did not show sexual dimorphism in any of the four views of the cranium. The clear change in shape based on the age and dental class on all four sides of the cranium describes the development, which showed the most change in the mandible with a p-value < 0.0001 in age, and a p-value of 0.0004 in class (Table 5). For the juveniles, the CV1 and CV2 had the highest value, while in the subadults the value of the CV1 was higher and the value for the CV2 was lower. On the contrary, the CV1 value for the adults was lower while the CV2 value was highest. The dental classes showed a similar pattern (Figure 7).

The *C. chacoensis* showed sexual dimorphism in all four views of the cranium (Table 5). The general development pattern showed a change on all sides of the cranium, with a p-value of < 0.0001, where CV1 and CV2 showed a similar relationship in the dorsal, mandible, and ventral sides where CV1 was higher on adults, while CV2 was kept at the same range. The juveniles were usually in the lower range for CV1 and variated from high to low values of CV2. The subadults were the exception with variation on all sides of the skull. On the contrary, on the lateral side, the juveniles and subadults were in the higher range on CV1 while the adults were in the lower range. The three variables were kept in the same range for CV2. On the other hand, the age classes on all sides of the skull were kept in the same range of CV2. On CV1, classes 1 to 3 were in the lower range while classes 6 to 7 were in the higher range on all sides of the skull. The only exception was the subadults which variated on all sides of the skull. Regarding the sex, on the lateral, mandible, and ventral sides most males had a frequency of 1, while on the dorsal side, the frequency variated between 1 and 3. The CV1 was in the lower range for the dorsal, lateral, and ventral sides, and in the higher range for the mandible. The females showed a similar pattern of occurrence to the males with few exceptions where some specimens had a higher frequency than average. On the contrary, the females had a higher range in CV1 than the males on the dorsal, lateral, and ventral sides, while in the mandible, the CV1 range was lower than the males. The results can be visualized in Figure 5 and Figure 8.

Allometric studies on Didelphids have shown that the size of their rostrum is more associated with their food habits rather than their size per se as its morphology is associated with feeding biomechanics (Flores et al. 2022). These studies have shown that the advantage of masticatory muscles is related to the length of the rostrum and the jaw, as well as to the position of the articular condyle and the coronoid process (Flores et al. 2022). In *C. chacoensis*, the most posteroventral point of the occipital condyle on the mandible showed variation depending on sex, age, and class groups (Appendix A, Figures 5 and 8), while in *G. agilis* (Appendix A, Figures 4 and 7) the length of this point shows a slight dimorphism in all three variables (sex, age, and class group). Similarly, on the mandible side of *C. chacoensis*, landmarks 6, 8, 9, 10, and 11 (Figure 2) which are related to the coronoid process and the articular condyle (Appendix A, Figures 5 and 8) show a strong dimorphism of length and width in all three variants of sex, age, and class group. On *G. agilis* there is barely any variation on these points (Figures 4 and 7). Nonetheless, even small changes in the growth pattern of the rostral and the mandible show important mechanical implications of both biting and chewing (Flores et al. 2022), which is evident in *C. chacoensis*, but barely perceptible in *G. agilis* (Figures 4 and 5). Furthermore, a short muzzle is observed on *C. chacoensis*, but not in *G. agilis*. This characteristic is associated with the mechanical efficiency of biting, as a short and robust cranium allows a stronger bite force and a high mechanical advantage within canines, the middle molar, and the posterior molar. This pattern is also observed in hyenas, felids, and other carnivore placentals (Flores et al. 2022). Furthermore, in other mammals, longer rostrums are highly associated with insectivory (Samuels 2009; Maestri et al. 2016).

The Procrustes allometric regression analysis showed that there is a positive allometric trend out of isometry on all sides of both species, where the relative size of these views increases. This is especially evident on the ramus part of the mandible of *C. chacoensis*. Nonetheless, the body part of the mandible seems to retract, showing a negative allometric trend (Figure 9).

Subsequently, the relation of shape as a function of size is stronger on the mandible of *G. agilis*, as well as in the dorsal and ventral view of both species (Table 6 & Figure 9).

Studies on *G. agilis* and *C. chacoensis* have primarily used linear morphometrics; nonetheless, these species have generally not been fully analyzed at a more in-depth level. A continuous problem encountered using traditional morphometrics includes the analysis of species that have small proportions such as rostrums and orbits, which prevents conclusive morphometric analysis (Voss et al. 2005). This problem of size does not pose a problem in geometric morphometrics due to being landmark based, which shows a more in-depth study of the allometric relationship between species. This variability problem is usually caused by the reduced number of specimens in museum collections (Garcia et al. 2010). Similarly, this problem also includes the lack of sexual and age variation within the current samples of *G. agilis*. By increasing the number of samples, the gaps between sex variations would change. Nonetheless, the patterns of sexual dimorphism may vary locally. This lack of variation could also be caused by the semelparity nature of *G. agilis* (Lopes and Leiner 2015) where the males of a group die after a short breeding season, but some females survive to reproduce for a second time (Cockburn 1997; Oakwood et al. 2001; Jones et al. 2003). Increasing the number and variation of samples of these specimens is necessary to study their ontological differences and ecology on a deeper level, as well as to further our understanding of these species in all stages of development. A low correlation between the skull shape of larger Didelphidaes and their diet has been identified, but further studies need to be made on the smaller species (Lemos et al. 2001).

In general, geometric morphometrics proves to be a useful tool for studying the skull allometry of these smaller marsupials. Consequently, analyzing the correlation between these shapes and their diet is valuable to better understand biodiversity.

ACKNOWLEDGMENTS

I would like to thank the staff at the mammal division at the Field Museum for access to their collection and for all the work they do to maintain these valuable resources including Adam Ferguson, Anderson Feijo, Lauren Smith, Lauren Nassef, John Phelps, and Lawrence Heaney. I would also like to thank all Paraguay field crews who helped collect specimens, especially Pastor E. Perez, Lourdes Valdez, Maria Luisa Ortiz, Julio Torres, and Mario Maldonado. Sarah Boyle, Fredy Ramirez, and Myriam Velazquez were pivotal with getting samples from Tapyta. I am forever grateful to the Environmental Sciences and Studies department at DePaul University for helping me during my research, including Dr. James Montgomery, who lent me his knowledge at the beginning of this research, and Dr. Christie Klimas, who was a great support. Finally, I thank Dr. Noé U. de la Sancha for his help, guidance, and support in completing this project.

REFERENCES

Abdala, F., D. A. Flores, and N. P. Giannini. 2001. Postweaning Ontogeny of the Skull of *Didelphis albiventris*. Journal of Mammalogy 82:190–200.

Adams, D. C., and A. Nistri. 2010. Ontogenetic Convergence and Evolution of Foot Morphology in European Cave Salamanders (Family: Plethodontidae). BMC Evolutionary Biology 10:216.

Adams, D. C., and E. Otárola-Castillo. 2013. Geomorph: An R Package for the Collection and Analysis of Geometric Morphometric Shape Data. Methods in Ecology and Evolution / British Ecological Society 4:393–399.

Astua, D. 2010. Cranial Sexual Dimorphism in New World Marsupials and a Test of Rensch's Rule in Didelphidae. Journal of Mammalogy 91:1011–1024.

Astúa, D. 2015. Morphometrics of the Largest New World Marsupials, Opossums of the Genus Didelphis (Didelphimorphia, Didelphidae). Oecologia Australis 19:117–142.

Astúa de Moraes, D., E. Hingst-Zaher, L. Marcus, and R. Cerqueira. 2000. A Geometric Morphometric Analysis of Cranial and Mandibular Shape Variation of Didelphid Marsupials. Hystrix-the Italian Journal of Mammalogy 11.

Astúa, D., and G. Guilhon. 2022. Morphology, Form, and Function in Didelphid Marsupials. In N. C. Cáceres, C. R. Dickman, eds. American and Australasian Marsupials: An Evolutionary, Biogeographical, and Ecological Approach. Springer International Publishing, Cham. p. 1–31.

Boyle, S. A., N. U. de la Sancha, P. Pérez, and D. Kabelik. 2021. Small Mammal Glucocorticoid Concentrations Vary with Forest Fragment Size, Trap Type, and Mammal Taxa in the Interior Atlantic Forest. Scientific Reports 11:2111.

Cardini, A. 2016. Lost in the Other Half: Improving Accuracy in Geometric Morphometric Analyses of One Side of Bilaterally Symmetric Structures. Systematic Biology 65:1096–1106.

Chemisquy, M. A., S. D. Tarquini, C. O. Romano Muñoz, and F. J. Prevosti. 2021. Form, Function, and Evolution of the Skull of Didelphid Marsupials (Didelphimorphia: Didelphidae). Journal of Mammalian Evolution 28:23–33.

Clark, C. T., and K. K. Smith. 1993. Cranial Osteogenesis in *Monodelphis domestica* (Didelphidae) and *Macropus eugenii* (Macropodidae). Journal of Morphology 215:119–149.

Cockburn, A. 1997. Living Slow and Dying Young: Senescence in Marsupials. Marsupial Biology: Recent Research, New Perspectives. University of New South Wales Press, Sydney:163–171.

Costa, L. P., Y. L. R. Leite, and J. L. Patton. 2003. Phylogeography and Systematic Notes on Two Species of Gracile Mouse Opossums, Genus Gracilinanus (Marsupialia: Didelphidae) from Brazil. Proceedings-Biological Society.

Coues, E. 1872. On the Osteology and Myology of *Didelphys virginiana.* Boston Society of Natural History.

Damasceno, E. M., and D. Astúa. 2016. Geographic Variation in Cranial Morphology of the Water Opossum *Chironectes minimus* (Didelphimorphia, Didelphidae). Mammalian Biology = Zeitschrift fur Saugetierkunde 81:380–392.

Diogo, R., J. M. Ziermann, J. Molnar, N. Siomava, and V. Abdala. 2018. Muscles of Chordates: Development, Homologies, and Evolution. CRC Press.

Drake, A. G. 2011. Dispelling Dog Dogma: An Investigation of Heterochrony in Dogs Using 3D Geometric Morphometric Analysis of Skull Shape. Evolution & Development 13:204–213.

Eisenberg, J. F., and D. E. Wilson. 1981. Relative Brain Size and Demographic Strategies in Didelphid Marsupials. The American Naturalist 118:1–15.

Flores, D. A., F. Abdala, and N. Giannini. 2010. Cranial Ontogeny of *Caluromys philander* (Didelphidae: Caluromyinae): A Qualitative and Quantitative Approach. Journal of Mammalogy 91:539–550.

Flores, D. A., F. Abdala, and N. P. Giannini. 2013. Post-weaning Cranial Ontogeny in Two Bandicoots (Mammalia, Peramelomorphia, Peramelidae) and Comparison with Carnivorous Marsupials. Zoology 116:372–384.

Flores, D. A., F. Abdala, and N. P. Giannini. 2022. Postweaning Skull Growth in Living American and Australasian Marsupials: Allometry and Evolution. In N. C. Cáceres, C.R. Dickman, eds. American and Australasian Marsupials: An Evolutionary, Biogeographical, and Ecological Approach. Springer Naturem Cham, Switzerland. p. 1–45

Flores, D. A., F. Abdala, and N. P. Giannini. 2023. Postweaning Skull Growth in Living American and Australasian Marsupials: Allometry and Evolution. In N. C. Cáceres, C.R. Dickman, eds. American and Australasian Marsupials: An Evolutionary, Biogeographical, and Ecological Approach. Springer Nature, Cham, Switzerland. p. 358–385.

Flores, D. A., F. Abdala, G. M. Martin, N. P. Giannini, J. M. Martinez, and Grupo Mastozoología. 2015. Post-Weaning Cranial Growth in Shrew Opossums (Caenolestidae): A Comparison with Bandicoots (Peramelidae) and Carnivorous Marsupials. Journal of Mammalian Evolution 22:285–303.

Flores, D. A., and L. Barone. 2012. Cranio-Facial Sutures of the Black-Capped Squirrel Monkey *Saimiri boliviensis* (Primates: Cebidae): Gross Morphology and Postnatal Ontogeny. Mammalia 76:91–98.

Flores, D. A., N. Giannini, and F. Abdala. 2006. Comparative Postnatal Ontogeny of the Skull in the Australidelphian Metatherian *Dasyurus albopunctatus* (Marsupialia: Dasyuromorpha: Dasyuridae). Journal of Morphology 267:426–440.

Flores, D. A., N. Giannini, and F. Abdala. 2018. Evolution of Post-weaning Skull Ontogeny in New World Opossums (Didelphidae). Organisms, Diversity & Evolution 18:367–382.

Fonseca, R., and D. Astúa. 2015. Geographic Variation in *Caluromys derbianus* and *Caluromys lanatus* (Didelphimorphia: Didelphidae). Zoologia 32:109–122.

Freeland, W. J., and D. H. Janzen. 1974. Strategies in Herbivory by Mammals: The Role of Plant Secondary Compounds. The American Naturalist 108:269–289.

Fritz, J., J. Hummel, E. Kienzle, C. Arnold, C. Nunn, and M. Clauss. 2009. Comparative Chewing Efficiency in Mammalian Herbivores. Oikos 118:1623–1632.

Garcia, J. P., J. A. Oliveira, M. M. O. Corrêa, and L. M. Pessôa. 2009. Morphometrics and Cytogenetics of *Gracilinanus agilis* and Cryptonanus spp. (Didelphimorphia: Didelphidae) from Central and Northeastern Brazil. Journal of Neotropical Mammalogy.

Garcia-Perea, R. 1996. Patterns of Postnatal Development in Skulls of Lynxes, Genus Lynx (Mammalia: Carnivora). Journal of Morphology 229:241–254.

Gardner, A. L. 1973. The Systematics of the Genus Didelphis (Marsupialia: Didelphidae) in North and Middle America. Special Publications Museum Texas Tech University 4:1–81.

Giannini, N. P., F. Abdala, and D. A. Flores. 2004. Comparative Postnatal Ontogeny of the Skull in *Dromiciops gliroides* (Marsupialia: Microbiotheriidae). American Museum Novitates 3460:1.

Giannini, N. P., V. Segura, M. I. Giannini, and D. Flores. 2010. A Quantitative Approach to the Cranial Ontogeny of the Puma. Mammalian Biology = Zeitschrift fur Saugetierkunde 75:547–554.

Hair, J. F., J. F. Hair Jr, R. E. Anderson, and R. L. Tatham. 1987. Multivariate Data Analysis with Readings. Macmillan.

Hernandez, G., S. Garcia, J. F. Vilela, and N. U. de la Sancha. 2017. Ontogenetic Variation of an Omnivorous Generalist Rodent: the Case of the Montane Akodont (*Akodon montensis*). Journal of Mammalogy 98:1741–1752.

Hiiemae, K., and F. A. Jenkins. 1969. The Anatomy and Internal Architecture of the Muscles of Mastication in Didelphis Marsupialis. Peabody Museum of Natural History.

Jones, M., M. Archer, and C. Dickman. 2003. Predators with Pouches: The Biology of Carnivorous Marsupials. Csiro Publishing.

Klingenberg, C. P. 1998. Heterochrony and Allometry: The Analysis of Evolutionary Change in Ontogeny. Biological Reviews of the Cambridge Philosophical Society 73:79–123.

Klingenberg, C. P. 2011. MorphoJ: An Integrated Software Package for Geometric Morphometrics. Molecular Ecology Resources 11:353–357.

Klingenberg, C. P. 2016. Size, Shape, and Form: Concepts of Allometry in Geometric Morphometrics. Development Genes and Evolution 226:113–137.

La Croix, S., K. E. Holekamp, J. A. Shivik, B. L. Lundrigan, and M. L. Zelditch. 2011a. Ontogenetic Relationships Between Cranium and Mandible in Coyotes and Hyenas. Journal of Morphology 272:662–674.

La Croix, S., M. L. Zelditch, J. A. Shivik, B. L. Lundrigan, and K. E. Holekamp. 2011b. Ontogeny of Feeding Performance and Biomechanics in Coyotes. Journal of Zoology 285:301–315.

Lopes, G. P., and N. O. Leiner. 2015. Semelparity in a Population of *Gracilinanus agilis* (Didelphimorphia: Didelphidae) Inhabiting the Brazilian Cerrado. Mammalian Biology = Zeitschrift fur Saugetierkunde 80:1–6.

Maestri, R., B. D. Patterson, R. Fornel, L. R. Monteiro, and T. R. O. de Freitas. 2016. Diet, Bite Force and Skull Morphology in the Generalist Rodent Morphotype. Journal of Evolutionary Biology 29:2191–2204.

Maunz, M., and R. Z. German. 1996. Craniofacial Heterochrony and Sexual Dimorphism in the Short-Tailed Opossum (*Monodelphis domestica*). Journal of Mammalogy 77:992–1005.

Oakwood, M., A. J. Bradley, and A. Cockburn. 2001. Semelparity in a Large Marsupial. Proceedings. Biological sciences / The Royal Society 268:407–411.

de Oliveira, C. A., J. C. Nogueira, and G. A. Mahecha. 1998. Sequential Order of Appearance of Ossification Centers in the Opossum *Didelphis albiventris* (Didelphidae) Skeleton During Development in the Marsupium. Annals of Anatomy = Anatomischer Anzeiger: Official Organ of the Anatomische Gesellschaft 180:113–121.

Osgood, W. H. 1921. A Monographic Study of the American Marsupial, Caenolestes. University of Chicago.

Pacini, N., and D. M. Harper. 2008. Aquatic, Semi-Aquatic and Riparian Vertebrates. In D. Dudgeon, ed. Tropical Stream Ecology (D. Dudgeon, ed.). Academic Press, London. p. 147–197.

Pilatti, P., and D. Astúa. 2017. Orbit Orientation in Didelphid Marsupials (Didelphimorphia: Didelphidae). Current Zoology 63:403–415.

Rohlf, F. J. 2015. The TPS series of software. Hystrix 26:9–12.

Samuels, J. X. 2009. Cranial Morphology and Dietary Habits of Rodents. Zoological Journal of the Linnean Society 156:864–888.

de la Sancha, N. U. 2014. Patterns of Small Mammal Diversity in Fragments of Subtropical Interior Atlantic Forest in Eastern Paraguay. Mammalia 78:437–449.

Sebastião, H., and G. Marroig. 2013. Size and Shape in Cranial Evolution of Two Marsupial Genera: Didelphis and Philander (Didelphimorphia, Didelphidae). Journal of Mammalogy 94:1424–1437.

Segura, V. 2013. Skull Ontogeny of *Lycalopex culpaeus* (Carnivora: Canidae): Description of Cranial Traits and Craniofacial Sutures. Mammalia 77.

Segura, V. 2015. A Three-Dimensional Skull Ontogeny in the Bobcat (*Lynx rufus*) (Carnivora: Felidae): A Comparison with Other Carnivores. Canadian Journal of Zoology.

Segura, V., and D. A. Flores. 2009. Aproximación Cualitativa y Aspectos Funcionales en la Ontogenia Craneana de *Puma concolor* (Felidae). Mastozoologia Neotropical 16:169–182.

Segura, V., F. Prevosti, and G. Cassini. 2013. Cranial Ontogeny in the Puma Lineage, *Puma concolor*, *Herpailurus yagouaroundi,* and *Acinonyx jubatus* (Carnivora: Felidae): A Three-Dimensional Geometric Morphometric Approach. Zoological Journal of the Linnean Society 169:235–250.

Sharp, A. C. 2015. Comparative Finite Element Analysis of the Cranial Performance of Four Herbivorous Marsupials. Journal of Morphology 276:1230–1243.

Smith, K. K. 2006. Craniofacial Development in Marsupial Mammals: Developmental Origins of Evolutionary Change. Developmental Dynamics: An Official Publication of the American Association of Anatomists 235:1181–1193.

Tomo, S., I. Tomo, G. C. Townsend, and K. Hirata. 2007. Masticatory Muscles of the Great-gray Kangaroo (*Macropus giganteus*). Anatomical Record 290:382–388.

Tribe, C. J. 1990. Dental Age Classes in *Marmosa incana* and Other Didelphoids. Journal of Mammalogy 71:566–569.

Ventura, J., M. Salazar, R. Pérez-Hernández, and M. J. López-Fuster. 2002. Morphometrics of the Genus Didelphis (Didelphimorphia: Didelphidae) in Venezuela. Journal of Mammalogy 83:1087–1096.

Voss, R. S., and S. A. Jansa. 2009. Phylogenetic Relationships and Classification of Didelphid Marsupials: An Extant Radiation of New World Metatherian Mammals. Bulletin of the American Museum of Natural History 322:1–177.

Voss, R. S., D. P. Lunde, and S. A. Jansa. 2005. On the Contents of Gracilinanus Gardner and Creighton, 1989, with the Description of a Previously Unrecognized Clade of Small Didelphid Marsupials. American Museum Novitates 3482:1–36.

Weisbecker, V., A. Goswami, S. Wroe, and M. R. Sánchez-Villagra. 2008. Ossification Heterochrony in the Therian Postcranial Skeleton and the Marsupial–Placental Dichotomy. Evolution 62:2027–2041.

Wroe, S., and N. Milne. 2007. Convergence and Remarkably Consistent Constraint in the Evolution of Carnivore Skull Shape. International Journal of Organic Evolution 61:1251–1260.

Zelditch, M., D. Swiderski, and H. David Sheets. 2012. Geometric Morphometrics for Biologists. Academic Press.

APPENDIX

Appendix A. Definition of landmarks from Figure 1 and Figure 2.

Dorsal view of the cranium. 1: Tip of the nasal; 2: Posterior end of the left and right junction of nasal; 3: Junction between right and left suture of frontal and parietal bones; 4: Posterior end of the interparietal bone, on the intersection of the sagittal line with the nuchal crest; 5: Squamosal curving point at the beginning of the nuchal crest anterior to the post-tympanic process; 6: Contact point between the zygomatic arch and parietal bone; 7: Distal posterior-most of the zygomatic arch; 8: Anterior end of the suture between the nasal bone and the premaxilla; 9: Intersection of sutures between nasal and frontal bones and maxilla; 10: Most anterior point of the orbit; 11: Intersection between the anterior rim of the squamosal process that forms the zygomatic arch and the rim of the braincase.

Ventral view of the cranium. 1: Anterior-most end of palate between incisors; 2: Posterior-most end of palate; 3: Anterior-most point of the foramen magnum (ventral view); 4: Posterior-most point of the occipital condyle; 5: Contact point between paroccipital process and pars mastoid; 6: Distal-most point of connection between the tempanic wing of alisphenoid and ectotympanic; 7: Posterior-most point of suture between jugal and squamosal; 8: Point of maximum curvature on anterior margin of zygomatic process of the temporal bone; 9: Posterior distal-most corner of palate; 10: Posterior-most end of M4; 11: Distal-most point between M3 and M4; 12: Distal-most point between M1 and P3; 13: Distal-most point between canine and P1; 14: Anterior-most point of I5.

Lateral view of the cranium. 1: Anterior base of the first superior incisive; 2: Posterior base of the fifth superior incisive; 3: Anterior base of the superior canine, on the maxillary bone junction with the tooth; 4: Posterior base of the superior canine, on the maxillary bone junction with the tooth; 5: Base of the third premolar and the first superior molar; 6: Posterior base of M4, where the tooth meets the maxillary bone (posterior end of the molar series); 7: Most posteroventral point of the occipital condyle; 8: Most posteroventral point of the braincase (posterior end of the sagital line, junction with the nuchal crest); 9: Top of the sagittal crest, where the frontal and pariental bones meet; 10: Point of contact between antorbital bridge (or maximillary) and lacrimal; 11: Junction of the nasal, premaxillary and maxillary bones sutures; 12: Anterior end of the sutures between the nasal and premaxillary bones; 13: Most anterior point of the orbit; 14: Jugal bone's frontal process end, on the zygomatic arch.

Mandible. 1: Base of the first inferior incisive; 2: Base of the fourth inferior incisive; 3: Posterior end of the inferior canine alveoli; 4: Base of the third premolar and the first molar where the teeth encounters the dentary bone; 5: Posterior base of the inferior fourth molar, where the teeth encounters the dentary bone; 6: Where the horizontal ramus of the mandible and beginning of the coronoid process meets (base of the coronoid process); 7: Anterior end of coronoid process; 8: Highest point of the coronoid process; 9: Posterior end of the coronoid process (beginning of the posterior edge of the coronoid process); 10: Point of biggest inflexion of the curvature between the articular process and the posterior edge of the coronoid process (base of the posterior edge); 11: Lateral end of the articular condyle; 12: Posterior base of the angular process; 13: Tip of the angular process; 14: Anterior base of the angular process; 15: Projection of point 5 on the ventral edge of the mandible, perpendicular to the line formed by point 4 and 5; 16: Projection of point 4 on the ventral edge of the mandible perpendicular to the line formed by point 4 and 5; 17: Projection of point 3 on the ventral edge of the mandible; 18: Anteroventral end of masseteric fossa; 19: Upper end part of mental foramen.

Appendix B. Results of the PCA analysis for the PC1 and PC2 loading based on landmarks for the four views on *G. agilis* and *C. chacoensis*. The PC loadings were illustrated based on the criteria of (Hair et al. 1987), where the values with >0.30 and <-0.30 are important (*), and the PC loadings with >0.50 and <0.50 are highly important (**).

Position of Landmarks	*Gracilinanus agilis*								*Cryptonanus chacoensis*							
	Dorsal		Mandible		Lateral		Ventral		Dorsal		Mandible		Lateral		Ventral	
	PC1	PC2	PC1	PC2	PC1	PC2	PC1	PC2	PC1	PC2	PC1	PC2	PC1	PC2	PC1	PC2
x1	-0.29	0.09	0.07	0.11	-0.12	0.05	0.19	0.09	-0.38*	0.27	-0.19	-0.07	0.09	-0.07	0.23	0.33*
y1	0.01	0.01	0.07	0.11	0.03	-0.07	0.07	-0.03	0.03	0.01	-0.10	0.14	0.05	-0.03	0.08	-0.19
x2	0.49*	0.15	-0.03	0.10	-0.27	-0.03	-0.01	-0.10	0.36*	-0.29	-0.09	-0.03	0.08	0.21	0.04	0.01
y2	-0.01	0.07	0.07	0.15	-0.05	-0.08	0.25	-0.13	-0.04	-0.08	-0.14	0.14	0.02	0.01	0.25	0.16
x3	0.00	-0.86**	-0.02	-0.01	-0.25	-0.01	0.38*	0.09	0.40*	0.72**	-0.06	-0.05	0.02	0.18	0.09	-0.02
y3	-0.23	-0.06	0.07	0.15	-0.18	-0.06	0.35*	-0.21	-0.14	0.12	-0.14	0.04	-0.02	0.11	0.33*	0.02
x4	-0.22	0.10	0.16	-0.40*	-0.21	-0.01	-0.11	0.24	-0.31*	-0.10	0.03	-0.19	0.01	0.22	-0.13	0.22
y4	-0.34*	-0.08	-0.01	-0.13	-0.12	-0.09	0.16	-0.11	-0.30	0.07	-0.04	0.00	0.01	0.08	0.12	-0.66**
x5	-0.09	0.31*	-0.53**	-0.14	0.18	-0.14	-0.07	0.18	-0.18	-0.13	0.50**	0.13	0.04	-0.29	0.05	0.04
y5	0.16	0.05	-0.09	-0.10	-0.12	-0.02	-0.15	0.01	0.07	-0.05	0.05	-0.09	-0.04	0.20	-0.16	-0.06
x6	0.11	0.16	-0.18	-0.02	0.32*	-0.56**	0.25	-0.13	0.07	-0.01	0.15	0.05	0.33*	-0.10	0.13	-0.18
y6	0.24	0.01	0.05	-0.05	0.23	-0.13	-0.18	0.01	0.18	0.03	-0.09	-0.23	0.09	-0.07	-0.16	0.06
x7	0.12	-0.05	0.25	0.14	0.06	0.08	0.12	-0.06	0.15	0.03	-0.23	0.16	-0.04	-0.31*	0.07	-0.12
y7	0.06	-0.16	0.04	0.18	0.14	0.24	-0.14	0.12	0.14	-0.04	0.10	-0.02	-0.06	-0.28	-0.07	0.16
x8	-0.35*	-0.04	0.24	0.07	-0.17	-0.15	0.13	0.06	-0.24	0.12	-0.20	0.16	0.03	0.16	0.32*	0.07
y8	0.09	0.03	0.00	0.16	-0.14	-0.01	-0.32*	0.05	0.05	-0.03	0.08	-0.04	-0.05	0.20	-0.16	0.23
x9	-0.32*	-0.11	0.17	-0.02	-0.30	0.39*	-0.09	-0.15	0.23	-0.46**	-0.24	0.35*	0.07	0.10	-0.07	0.03
y9	-0.12	0.07	-0.07	0.09	-0.32*	-0.37*	-0.03	0.11	-0.09	0.07	0.10	0.05	-0.05	0.45*	0.13	0.12
x10	-0.10	0.20	0.05	0.14	0.06	0.06	-0.18	-0.69**	-0.13	-0.06	-0.11	-0.02	0.16	0.00	0.18	-0.04
y10	-0.13	0.03	0.17	0.11	-0.04	0.16	-0.11	0.25	-0.16	-0.14	-0.13	0.07	0.05	0.04	-0.37*	0.15
x11	0.01	0.05	0.05	-0.11	0.29	0.03	-0.47*	-0.22	0.03	-0.09	-0.13	-0.09	-0.80**	-0.09	-0.29	-0.17
y11	0.25	0.02	0.05	-0.01	0.09	0.03	-0.01	0.00	0.27	0.03	-0.10	0.28	-0.15	-0.07	-0.08	0.18
x12	n/a	n/a	0.06	0.06	-0.02	0.12	-0.19	0.20	n/a	n/a	0.05	-0.04	0.18	-0.07	-0.46*	-0.21
y12	n/a	n/a	-0.10	0.05	0.09	-0.03	0.01	-0.01	n/a	n/a	0.13	-0.03	0.11	-0.19	-0.03	0.07
x13	n/a	n/a	0.15	-0.13	0.12	0.15	0.03	0.22	n/a	n/a	-0.16	-0.18	0.14	0.05	-0.03	-0.03
y13	n/a	n/a	-0.23	0.07	0.13	0.02	0.06	-0.03	n/a	n/a	0.12	-0.03	0.00	0.01	0.08	-0.06
x14	n/a	n/a	-0.23	0.27	0.30*	0.02	0.03	0.25	n/a	n/a	0.07	-0.47*	-0.30	-0.01	-0.13	0.08
y14	n/a	n/a	-0.05	-0.18	0.25	0.42*	0.05	-0.03	n/a	n/a	0.08	-0.14	0.05	-0.45*	0.04	-0.18
x15	n/a	n/a	-0.44*	-0.06	n/a	n/a	n/a	n/a	n/a	n/a	0.50*	0.42*	n/a	n/a	n/a	n/a
y15	n/a	n/a	-0.09	-0.18	n/a	n/a	n/a	n/a	n/a	n/a	0.07	-0.21	n/a	n/a	n/a	n/a
x16	n/a	n/a	0.19	-0.33*	n/a	n/a	n/a	n/a	n/a	n/a	0.00	0.08	n/a	n/a	n/a	n/a
y16	n/a	n/a	0.13	-0.15	n/a	n/a	n/a	n/a	n/a	n/a	-0.01	-0.01	n/a	n/a	n/a	n/a
x17	n/a	n/a	0.03	0.07	n/a	n/a	n/a	n/a	n/a	n/a	-0.12	0.04	n/a	n/a	n/a	n/a
y17	n/a	n/a	0.03	0.11	n/a	n/a	n/a	n/a	n/a	n/a	-0.01	0.04	n/a	n/a	n/a	n/a
x18	n/a	n/a	-0.11	0.30	n/a	n/a	n/a	n/a	n/a	n/a	0.22	-0.23	n/a	n/a	n/a	n/a
y18	n/a	n/a	-0.10	-0.40*	n/a	n/a	n/a	n/a	n/a	n/a	0.02	-0.04	n/a	n/a	n/a	n/a
x19	n/a	n/a	0.13	-0.04	n/a	n/a	n/a	n/a	n/a	n/a	0.00	-0.02	n/a	n/a	n/a	n/a
y19	n/a	n/a	0.05	0.01	n/a	n/a	n/a	n/a	n/a	n/a	0.00	0.08	n/a	n/a	n/a	n/a

Appendix C. List of some Old and New World marsupials to whom ontogenetic studies have been applied.

Old world marsupials: *Aepyprymnus rufescens, Ailurops ursinus, Antechinus stuartii, Bettongia penicillata, Cercartetus caudatus, Cercartetus nanus, Dasycercus byrnei, Dasycercus cristicauda, Dasyurus maculatus, Dasyurus viverrinus, Lagorchestes hirsutus, Lagostrophus fasciatus, Macropus giganteus, Macrotis lagotis, Murexechinus melanurus, Myrmecobius fasciatus, Neophascogale lorentzii, Notamacropus eugenii, Notamacropus rufogriseus, Onychogalea fraenata, Osphranter robustus, Petaurus breviceps, Petrogale penicillata, Phalanger orientalis, Phascogale tapoatafa, Phascolarctos cinereus, Planigale tenuirostris, Potorous tridactylus, Pseudocheirus peregrinus, Sarcophilus harrisii, Setonix brachyurus, Sminthopsis crassicaudata, Spilocuscus maculatus, Strigocuscus celebensis, Strigocuscus pelengensis, Tarsipes rostratus, Thylacinus cynocephalus, Thylogale billardierii, Thylogale stigmatica, Trichosurus vulpecula, Vombatus ursinus, Wallabia bicolor,* (Flores et al. 2022), *Dasyurus albopunctatus* (Flores et al. 2006), *Echymipera kalubu, and Isoodon macrourus* (Flores et al. 2013).

New world marsupials: *Chironectes minimus, Lutreolina crassicaudata, Marmosa demerarae, Marmosa murina, Marmosops incanus, Metachirus nudicaudatus, Monodelphis brevicaudata, Philander opossum, Thylamys sponsorius*, (Flores et al. 2018), *Didelphis albiventris* (Abdala et al. 2001), *Dromiciops gliroides* (Giannini et al. 2004), *Caluromys philander* (Flores et al. 2010), *Caenolestes fuliginosus, Lestoros inca, and Rhyncholestes raphanurus* (Flores et al. 2015).